

Photovoltaic laser power converter based on germanium

© O.A. Khvostikova, S.V. Sorokina, M.Z. Shvarts, B.Ya. Ber, D.Yu. Kasantsev, V.P. Khvostikov

Ioffe Institute,
194021 St. Petersburg, Russia
e-mail: svsorokina@mail.ioffe.ru

Received December 5, 2023

Revised March 13, 2024

Accepted March 14, 2024

The diffusion doping of germanium and design features of a photovoltaic converter for operation with high-power infrared laser radiation have been optimized. The chips are tested by using a uniform defocused and focused beam with the wavelength of 1550 nm. The monochromatic efficiency of $\sim 20\%$ (0.2 W) is achieved in the case of matching the spectral sensitivity of the converters to the operating wavelength of the laser.

Keywords: laser radiation, germanium, photovoltaic converter, diffusion, efficiency.

DOI: 10.61011/TP.2024.05.58525.297-23

Introduction

Laser radiation (LR) conversion is separate and quick developing direction in photovoltaic energetics covering an increasing number of semiconductor compounds and wavelengths [1–10]. The photovoltaic converters (PVC) of radiation of different wavelengths λ are used for remote power supply of portable electronics, household appliances and computer devices [11], re-charging of unmanned aerial vehicles/robots [12–14], wireless transmission of optical energy to self-contained [15] or remote object (including space one [16,17]) etc. Medical applications are becoming increasingly important — to increase service life of biological prostheses, medical sensors [18,19], cardiac stimulators and neurostimulators [20] implanted in patients. The areas of application of remote optical signal transmission with PVC participation are various and are constantly expanding. At that the problem „links“ of such systems stay the same — LR effective generation and its back conversion into electrical energy with minimum losses.

Germanium is widely distributed material of electronic engineering, it is characterized by developed industrial production and relatively low cost. The scientific literature of last years discusses the possibility of germanium PVC use during irradiation by LR with wavelengths 850 [21], 980 [22], 1310 [21] and 1550 nm [21, 22]. Special attention is paid to $\lambda = 1550$ nm entering the transparency windows of the atmosphere and optical fiber, which makes it possible to build open (through the atmosphere) wireless reception–transmission systems and long fiber-optic communication lines. Besides, for 1550 nm the effective erbium amplifiers are available, they can operate with optical signal practically without its distortion [23,24].

The monochromatic efficiency of germanium-based PVC LR for $\lambda = 1550$ nm significantly exceeds efficiency (η) of similar solar cells. Practically achieved values of η for spectrum AM1.5 are presented in Fig. 1 by lines 1–3 [25,26], monochromatic efficiency — by crimson

color histogram [21]. Maximum values of monochromatic efficiency of idealized PVC (yellow color histogram) for various LR wavelengths are given for photocurrent value $1 \text{ A}\cdot\text{cm}^2$. Calculations of idealized PVCs [27] did not consider losses for LR reflection from PVC surface, for shadowing by contacts, as well as recombination losses. From Fig. 1 it follows that nowadays achieved values of monochromatic efficiency of converters are significantly lower than the limit values. Assurance of high efficiencies at relatively simple converter structure and reproducible technology for its production will allow „exhibition“ of new application of the germanium and such PVC integration into wireless energy transmission systems via open channel or via optical fiber.

The present paper relates to adaptation of germanium-based PVC technology for wavelength of industrial laser

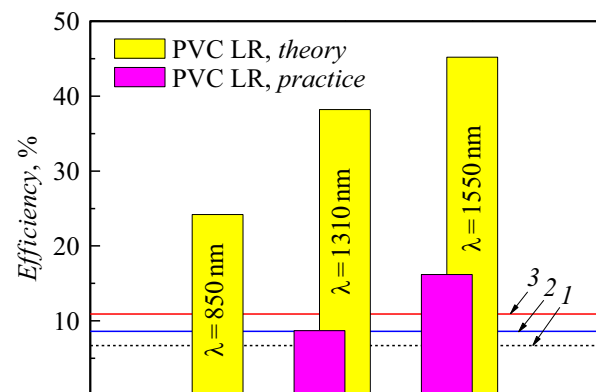


Figure 1. Histogram of efficiency values at wavelengths 850, 1310 and 1550 nm for idealized (yellow color, [27]) and practically implemented (crimson cover, [21]) PVC based on germanium. Dashed curves show efficiency values for solar cells: 1 — AM1.5, phosphorus diffusion in Ge [25]; 2, 3 — AM1.5, zinc diffusion into structures GaAs/Ge obtained by MOVPE and liquid-phase epitaxy [26].

with $\lambda = 1550$ nm and study of their possibilities upon irradiation by uniform and non-uniform incident LR.

1. Experiment

1.1. Features of technological process of PVC LR

Structures of PVC LR were formed by diffusion doping from gaseous phase. The process was performed in hydrogen stream, preventing substrates oxidation. Diffusion was carried out through a pre-formed dielectric mask (Si_3N_4 or SiO_2), protecting side surface of PVC against formation of p - n -transition (Fig. 2) and, hence, decreasing leak currents. Maximum of spectral response (SR) and minimum of reflection (R) antireflective coatings (ARC in Fig. 2) were matched to the wavelength of the incident radiation $\lambda = 1550$ nm. The choice of the dopant has been crucial. Value of spectral response of PVC (SR) was determined by the results of external quantum yield. Use of phosphine did not allow reproducible production of photosensitive structures with the required quality ($SR < 0.2$). Satisfactory values of spectral response were obtained using diborane B_2H_6 ($SR \leq 0.8$) or Sb ($SR \leq 0.8$, curve 1 Fig. 3, a). Significant increasing of SR was obtained during zinc

diffusion (Fig. 3, b). Limit values of spectral response were determined by expression $SR(\lambda) = \frac{q}{hc \cdot 1000} \lambda(nm) = \frac{\lambda(nm)}{1239.86}$.

1.2. Specific nature of doping with antimony

Diffusion of antimony and zinc was performed using a graphite box ensuring creation of quasi-uniform distribution of the diffuser vapors over the working surface of the substrate. During single stage doping with antimony (temperature 600°C , 30 min) we observed worsening of substrate morphology, which resulted further in significant decrease photocurrent PVC LR. Diffusion temperature decreasing reduced depth of p - n -junction, as result significant current leaks occurred. Meeting of conflicting requirements for structure and process were achieved by complicating the technological cycle and forming variable diffusion profile — with shallow ($0.3 \mu\text{m}$) emitter and local deep (0.7 – $1.0 \mu\text{m}$) p - n -junction under contacts (Fig. 2, b). Such two-stage technology was successfully used previously to receive solar cells based on GaSb [9,28,29]. Curves 1 and 2 in Fig. 3, a demonstrate values SR at single and two-stage diffusion process respectively. In last case the spectral response at 1550 nm is close to theoretical limit.

1.3. PVC optimization during doping with zinc

During doping with zinc high values of SR were reached even during single diffusion process (Fig. 3, b). Diffusion was performed at temperature 650 – 690°C .

Profiles of zinc distribution at different time of diffusion annealing were measured by method of dynamic secondary ion mass spectroscopy (D-SIMS) using secondary ion microprobe IMS-7f (CAMECA, France) using depth profiling. The primary ions were $^{16}\text{O}_2^+$ with kinetic impact energy on sample 5.5 keV, which focused on sample surface in the beam with diameter $20 \mu\text{m}$. Said beam scanned over sample surface the raster with size $200 \times 200 \mu\text{m}$. As secondary (analytical) ions we used ion of matrix $^{73}\text{Ge}^+$ and ion of dopant $^{64}\text{Zn}^+$. Only analytical ions emitted from central region of bottom ion etching crater with diameter $33 \mu\text{m}$. This suppressed the contribution to analytical signals of ions sputtered from crater walls on its bottom.

The depths of dopant concentration profiles were measured by speed of ion etching, for this using the mechanical stylus profilometer AMBIOS XP-1 (AMBIOS, USA) the total depth of ion etching crater was measured.

Quantitative analysis of zinc impurity content by through profile depth was carried out using the method of relative sensitivity coefficients [30] with correction to values of isotopic abundances for analytical isotopes ^{73}Ge and ^{64}Zn [31]. Results of D-SIMS of depth profiling of zinc distribution are presented in Fig. 4.

Theoretical estimation for diffusion from permanent source into semi-bounded body [32] is presented by dashed

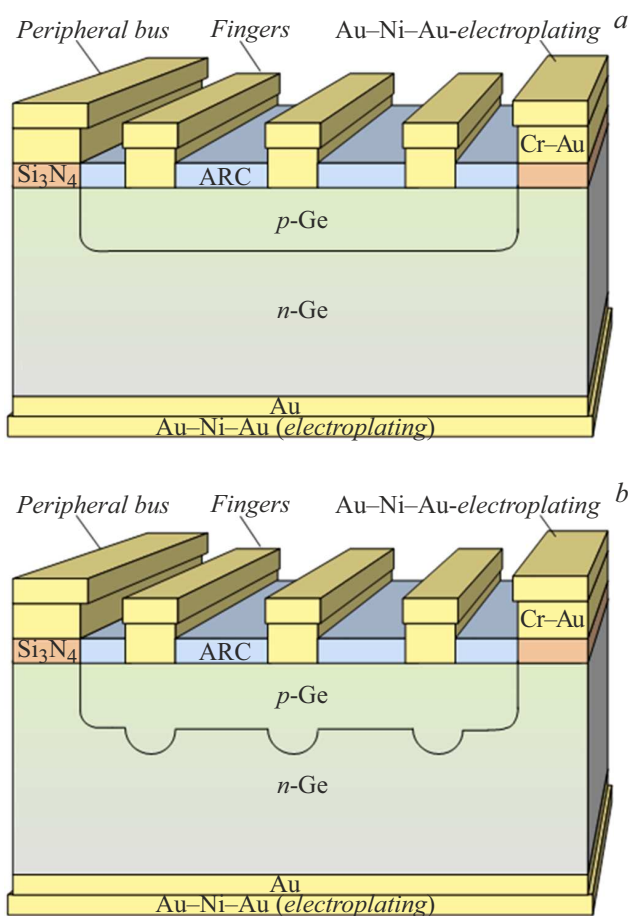


Figure 2. Structure of germanium-based PVC LR for single (a) and two-stage (b) diffusion.

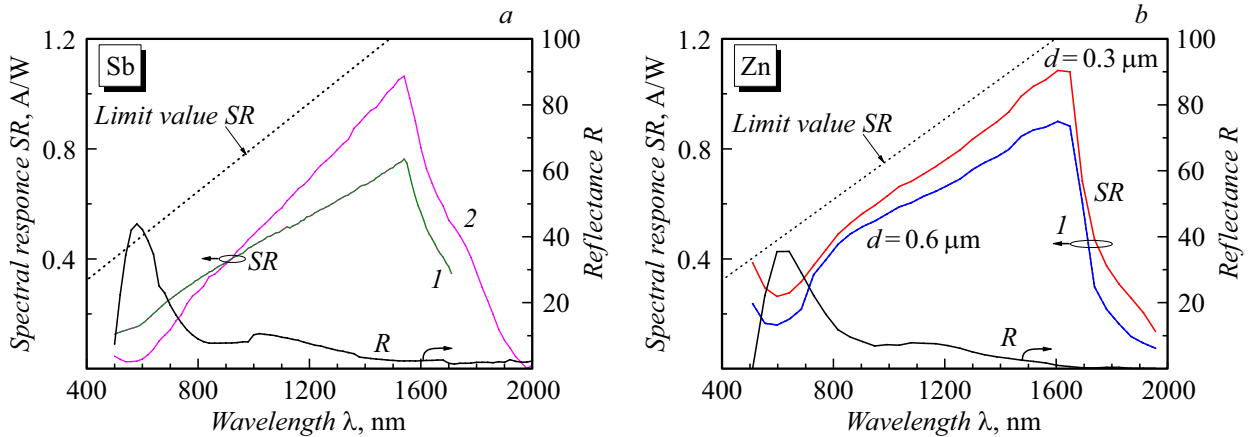


Figure 3. The spectral response of PVC upon doping with antimony (a) and zinc (b) during single (1) or two-stage (2) diffusion. For (b) depth of location of *p-n*-junction *d* is 0.3 and 0.6 μm.

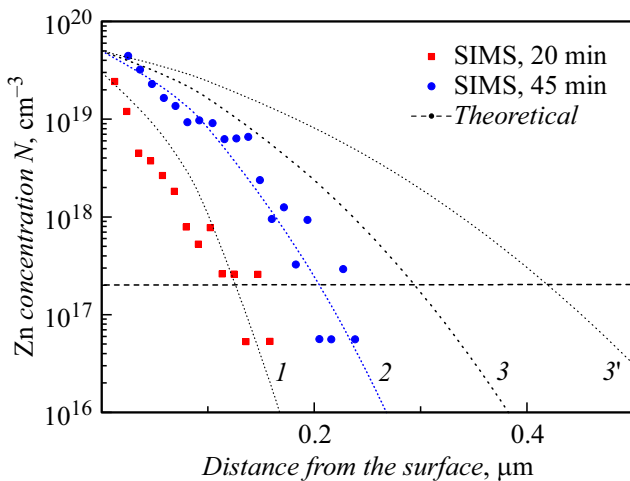


Figure 4. Theoretical distributions (dashed curves) and SIMS profiles (solid curves) of zinc in germanium at temperature 670°C. Time of diffusion annealing is: 1 – 20, 2 – 45, 3 – 90 min. Calculated curves are presented for $D \sim 11 \cdot 10^{-14} \text{ cm}^2/\text{s}$ (1–3) and for $D \sim 2 \cdot 10^{-14} \text{ cm}^2/\text{s}$ (3').

curves 1–3. Atoms distribution through depth of the semiconductor was estimated by formula

$$N = N_0 \operatorname{erfc} \left(\frac{x}{2\sqrt{Dt}} \right), \quad (1)$$

where diffusion coefficient was taken equal to $D \sim (1-2) \cdot 10^{-14} \text{ cm}^2/\text{s}$ [32]. Depth of *p-n*-junction was calculated if value of concentration of residual donors in substrate as substituted, and diffusion coefficient was assumed as independent of Zn concentration.

Final dependence of depth of location of *p-n*-junction on diffusion time at temperature 670°C is shown in Fig. 5. Data of measurements by scanning-electron microscopes Cam-Scan and JSM-35 are presented, as well as measurement results of SIMS and theoretical dependences for calculation

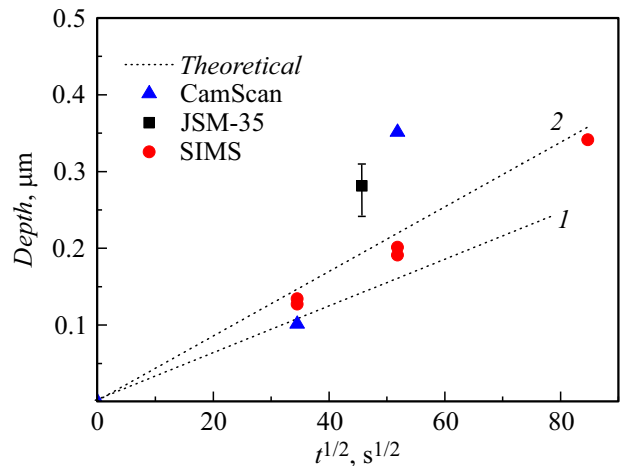


Figure 5. Depth of location of *p-n*-junction vs. diffusion time at temperature 670°C: 1 – $D = 1 \cdot 10^{-14}$, 2 – $2 \cdot 10^{-14} \text{ cm}^2/\text{s}$.

by formula (1) with diffusion coefficients $D \sim 1 \cdot 10^{-14}$ and $\sim 2 \cdot 10^{-14} \text{ cm}^2/\text{s}$.

Maximum efficiency and reproducibility of parameters of converters were obtained during zinc diffusion for ~ 35 min (depth of location of *p-n*-junction $\leq 0.3 \mu\text{m}$, data of JSM-35). For thinner emitters in PVC LR the leak currents increased during burning contacts. Besides, in case of shallow *p-n*-junction the open-circuit voltage is more critical to rate of surface recombination.

1.4. Design features of PVC LR

Ohmic contacts of PVC LR were created by sputtering of thin films Au or Cr–Au with subsequent galvanic build-up of metallization up to 1–3 μm by electrochemical deposition Au–Ni–Au (Fig. 2). To minimize the optical losses at the final stage of the technological process the two-layer antireflective coating ZnS–MgF₂ is applied, the reflection spectrum of which is shown by curves *R* in Fig. 3.

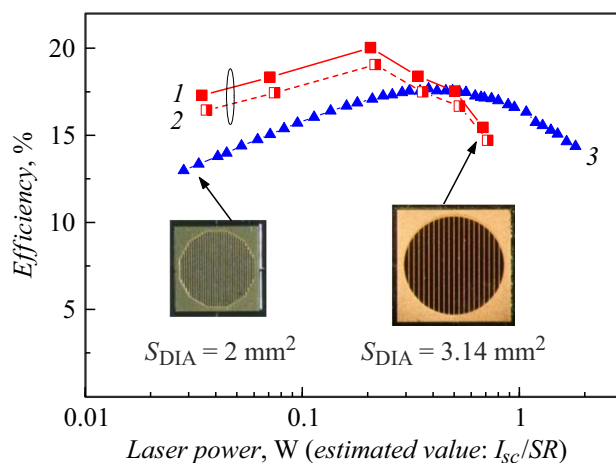


Figure 6. Monochromatic efficiency of PVC at uniform illumination, λ : 1, 3 — 1550, 2 — 1310 nm.

For effective energy reception-transmission in laser channels maximum possible densities of incident power will be necessary. Together with increase in efficiency, power of incident radiation (requiring, in turn, decrease in chip size and its series resistor) becomes an urgent technological problem. Diameter of light spot, obtained from the laser during samples testing, also was limited. So, chips with total size 2×2 mm and 2.5×2.5 mm were manufactured. Area for radiation supply (designated illumination area) S_{DIA} was 2 and 3.14 mm² respectively.

Configuration of contact mesh for both sizes of PVC was practically same — with equidistant (50 and 100 μ m respectively) location of contact strips (width 10 and 6 μ m respectively) inside a round photosensitive region and wide peripheral contact busbar (Fig. 6). S_{DIA} comprises area of thin contact strips. Periphery contact busbar is located beyond this zone [33]. With density increasing of power incident to the sample the role of ohmic losses increases, so, to decrease the series resistor of PVC with $S_{DIA} = 2$ mm² the interval of contact mesh decreased, and the shading coefficient increased from 6 to 20%.

For effective heat removal and to prevent overheating under action of powerful laser radiation PVC s were installed on heat conductive electric insulating boards of company „Rezonit“ made of aluminium alloy having dielectric layer and copper foil. Installation was performed using soldering paste based on alloy PbSnAg with melting point 180°C.

2. Results

The ideal optical system shall create a round light spot with uniform spatial distribution of incident power density in photoactive area of PVC. Any distortions of beam and mismatch of shape/geometric dimensions between the light spot and the converter will cause efficiency losses. In actual systems during LR transmission always definite unevenness of radiation is created on the surface of the converter (π -

like distribution for scattered radiation, Gaussian or close to it beam for single-mode and few-mode fibers [34], more complex profile for multimode light guide [35]). Besides, powerful LR will cause PVC heating and efficiency decreasing. So, in present paper the output parameters of chips were evaluated both in mode of uniform pulse illumination (xenon lamp, flash duration ~ 1.5 ms), and partially nonuniform irradiation (continuous wave laser with $\lambda = 1550$ nm with LR supply via optical fiber).

2.1. PVC efficiency during uniform LR

Pulse xenon lamp form uniform distribution of light flow on surface of photoconverter and successfully simulates radiation by laser without photodetector heating. Open-circuit voltage V_{oc} , short-circuit current I_{sc} , fill factor FF and efficiency vs. LR power for uniform illumination are presented in Fig. 6 and further in Fig. 8. Increased metalization thickness and small interval of frontal contact mesh ensured for the FF over 65%. At radiation power 0.2 W monochromatic ($\lambda = 1550$ nm) efficiency $\sim 20\%$ was achieved (Fig. 6, curve 1). Data are provided for the converter with diffusion doping with zinc, depth of location of p - n -junction 0.3 μ m and area $S_{DIA} = 3.14$ mm². Fig. 6 additionally contains dashed curve 2 for efficiency of said PVC at $\lambda = 1310$ nm ($\eta = 19.1\%$, 0.2 W). The optical signal transmission at wavelength 1310 nm, as in case $\lambda = 1550$ nm, is characterized by low losses (second fiber optic transparency window).

For similar converter with $S_{DIA} = 2$ mm² (Fig. 6, curve 3) maximum monochromatic ($\lambda = 1550$ nm) efficiency $\eta = 17.7\%$ is achieved at 0.5 W. Minor decrease in peak efficiency in this case is mainly associated with increase in shading coefficient of the photosensitive area (20% instead of 6%). At that the region of maximum efficiencies is shifted along density of supplied power from 5–7 W/cm² to 10–40 W/cm². The obtained values of the monochromatic efficiency noticeably exceed the earlier published practical results for $\lambda = 1550$ and 1310 nm ($\eta = 15.9$ and 8.5% [21] respectively).

2.2. PVC efficiency at non-uniform LR

When irradiating by laser with $\lambda = 1550$ nm two options of illumination were implemented:

- focused at center of converter by beam with Gaussian distribution of power (curve 1, Fig. 7). Radiation was supplied through optical fiber. Round light spot was characterized by large non-uniformity with intensity of illumination radially decreased to periphery (Fig. 7).

- defocused using an optical homogenizer by radiation with π -like profile of illumination distribution (curve 2, Fig. 7, light spot with diameter ~ 2 mm, low non-uniformity of LR).

For clarity inserts show graphical image of light spot on PVC surface, where change in intensity is illustrated by background coloring.

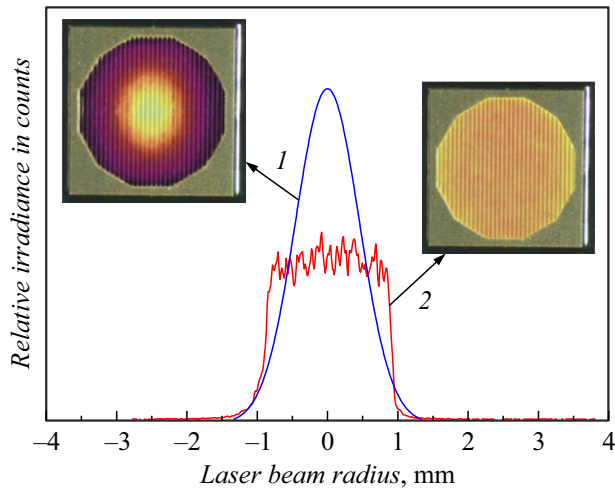


Figure 7. Distribution of laser beam radiation intensity: 1 — Gaussian distribution of power (focused laser beam); 2 — converted π -like profile (defocused laser beam).

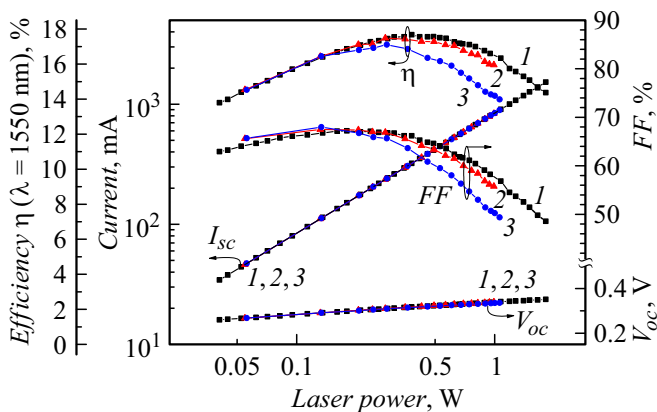


Figure 8. I_{sc} , V_{oc} , FF and efficiency of PVC ($S_{DIA} = 2.0 \text{ mm}^2$) vs. LR power: 1 — xenon lamp (uniform illumination), 2, 3 — illumination by laser beam ($\lambda = 1550 \text{ nm}$) with weak (π -like profile) and large (Gaussian distribution) non-uniformity respectively.

Supply of single light pulses of flash lamps do not cause radiative heating of PVC during recording of current-voltage curves and measuring of open-circuit voltage, this is confirmed by logarithmic growth V_{oc} with illumination up to values of incident power of LR 1 W. Similarly, irradiation by pulse laser with $\lambda = 1550 \text{ nm}$ does not result in significant radiation heating of the converter located on the heat sink and noticeable decrease in its V_{oc} . Data in Fig. 8 are presented by PVC illumination with $S_{DIA} = 2.0 \text{ mm}^2$. At incident power 0.4 W the converter demonstrates peak efficiency 17.7% (Xe lamp, uniform illumination, curve 1). Duration and period of laser pulses are 250 and 50000 μs respectively. Local inhomogeneity of illumination (focused laser beam) facilitates the decrease in FF and, hence, efficiency ($\Delta\eta = 2\%$ at 1 W, curves 3). Curves 2 show dependence of PVC output parameters on power when laser

radiation is unfocused over sample area. Use of optical homogenizer allows to reduce losses due to nonuniform laser irradiation, and to obtain efficiency over 17% at incident power 0.2–0.6 W.

Conclusion

The performed studies ensure to conclude that diffusion doping from gaseous phase with zinc ensures formation of qualitative p - n -junction and reproducible creation of photocell structures exceeding by spectral sensitivity the analogues with diffusion of diborane, phosphine and antimony. In case of uniform irradiation of low-size ($S_{DIA} = 3.14 \text{ mm}^2$) PVC based on germanium the monochromatic ($\lambda = 1550 \text{ nm}$) efficiency $\sim 20\%$ was obtained.

Acknowledgments

SIMS studies were carried out using the equipment of the Center for Collective Use „Materials Science and Diagnostics in Advanced Technologies“ (Ioffe FTI).

Conflict of interest

The authors declare that they have no conflict of interest.

References

- [1] C. Algora, I. García, M. Delgado, R. Pena, C. Vázquez, M. Hinojosa, I. Rey-Stolle. *Joule*, **6**, 1 (2021). DOI: 10.1016/j.joule.2021.11.014
- [2] M. Perales, M. Yang, C. Wu, C. Hsu, W. Chao, K. Chen, T. Zahuranec. *Proc. of SPIE-High-Power Diode Laser Technology and Applications XIV*, ed. by M.S. Zediker, vol. 9733, 97330U, 2016. DOI: 10.1117/12.2213886
- [3] S. Fafard, D.P. Masson. *J. Appl. Phys.*, **130** (16), 160901 (2021). DOI: 10.1063/5.0070860
- [4] H. Helmers, E. Lopez, O. Höhn, D. Lackner, J. Schön, M. Schauerte, M. Schachtner, F. Dimroth, A.W. Bett. *Phys. Status Solidi RRL*, **15** (7), 2100113 (2021). DOI: 10.1002/pssr.202100113
- [5] S. Fafard, D.P. Masson. *Photonics*, **9** (7), 438 (2022). DOI: 10.3390/photonics9070438
- [6] Y. Gou, H. Wang, J. Wang, Y. Zhang, R. Niu, X. Chen, B. Wang, Y. Xiao, Z. Zhang, W. Liu, H. Yang, G. Deng. *Optics Express*, **30** (23), 42178 (2022). DOI: 10.1364/OE.474693
- [7] V.P. Khvostikov, N.A. Kalyuzhnyy, S.A. Mintairov, N.S. Potapovich, O.A. Khvostikova, S.V. Sorokina, M.Z. Schwartz. *ZhTF*, **90** (10), 1764 (2020). (in Russian). DOI: 10.21883/JTF.2020.10.49811.43-20 [V.P. Khvostikov, N.A. Kalyuzhnyy, S.A. Mintairov, N.S. Potapovich, O.A. Khvostikova, S.V. Sorokina, M.Z. Shvarts. *Tech. Phys.*, **65** (10), 1690 (2020). DOI: 10.1134/S1063784220100096]
- [8] V.P. Khvostikov, N.A. Kalyuzhnyy, S.A. Mintairov, N.S. Potapovich, S.V. Sorokina, M.Z. Shvarts. *Semiconductors*, **53** (8), 1110 (2019). DOI: 10.1134/S1063782619080116

- [9] V.P. Khvostikov, S.V. Sorokina, F.Yu. Soldatenkov, N.Kh. Timoshina. *Semiconductors*, **49** (8), 1079 (2015). DOI: 10.1134/S1063782615080114
- [10] V.P. Khvostikov, A.N. Panchak, O.A. Khvostikova, P.V. Pokrovskiy. *IEEE Electron Device Lett.*, **43** (10), 1 (2022). DOI: 10.1109/LED.2022.3202987
- [11] J.D. López-Cardona, D.S. Montero, C. Vázquez. *IEEE Sensors J.*, **19** (17), 7328 (2019). DOI: 10.1109/JSEN.2019.2915613
- [12] V.A. Bogushevskaya, O.V. Zayats, Ya.N. Maslyakov, I.S. Matsak, A.A. Nikonov, V.V. Savelyev, A.A. Sheptunov. *Trudy MAI*, **51**, 1 (2012) (in Russian).
- [13] M.-A. Lahmeri, M.A. Kishk, M.-S. Alouini. *IEEE Transactions on Wireless Communications*, **22** (1), 518 (2023). DOI: 10.1109/TWC.2022.3195867
- [14] P. Anand, R. Pandiarajan, P. Raju. *J. Mechan. Eng. Research*, **5** (1), 137 (2015).
- [15] J. Mukherjee, W. Wulfken, H. Hartje, F. Steinsiek, M. Perren, S.J. Sweeney. *Proc. IEEE 39th Photovoltaic Specialists Conference* (2013). DOI: 10.1109/PVSC.2013.6744326
- [16] R.A. Evdokimov, V.Yu. Tugaenko, N.V. Shcherbenko. *Inzhenerny zhurnal: nauka i innovatsii*, **7**, 1 (2022). (in Russian). DOI: 10.18698/2308-6033-2022-7-2196
- [17] A. Sigov, V. Matyukhin. *Sovremennaya elektronika*, **1**, 18 (2015). (in Russian)
- [18] M. Mujeeb-U-Rahman, D. Adalian, Ch.-F. Chang, A. Scherer. *J. Biomed. Optics*, **20** (9), 095012 (2015). DOI: 10.1117/1.JBO.20.9.095012
- [19] A. Ahnood, R. Cheriton, A. Bruneau, J.A. Belcourt, J.P. Ndamakuranye, W. Lemaire, R. Hilkes, R. Fontaine, J.P.D. Cook, K. Hinzer, S. Prawerl. *Advance Biosystems.*, **4**, 2000055 (2020).
- [20] C. Algora, R. Peña. *Artificial Organs*, **33**(10), 855 (2009). DOI: 10.1111/j.1525-1594.2009.00803.x
- [21] G. Allwood, G. Wild, S. Hinckley. *Proc. Conference: Optoelectronic and Microelectronic Materials & Devices (COM-MAD)* (2012). DOI: 10.1109/COMMAD.2012.6472337
- [22] G. Allwood, G. Wild, S. Hinckley. *Proc. of SPIE — The International Society for Optical Engineering*, **8204**, 2011. DOI: 10.1117/12.903294
- [23] A.S. Kurkov, O.E. Nanij. *LIGHTWAVE Russ. Edition*, **1**, 14 (2003).
- [24] A.V. Dorofeenko, I.A. Nechepurenko, A.P. Bazakutsa, O.V. Butov. *Sovremennaya elektrodinamika*, **2** (4), 17 (2023). (in Russian)
- [25] N.E. Posthuma, J. van der Heide, G. Flamand, J. Poormans. *Proc. of the 6th Conference Thermophotovoltaic Generation of Electricity*, A. Gorpınath et al., eds. (Freiburg, Germany, 2004), p. 337–344. DOI:10.1063/1.1841911
- [26] O.A. Khvostikova. *Fotoelektricheskie preobrazovateli izlucheniya na osnove uzkozonnykh poluprovodnikov (GaSb, Ge, InAs)*: Dis. kand. fiz.-mat. nauk: 01.04.10 Khvostikova O.A. (SPb., 2009), 131 s. (in Russian)
- [27] A.V. Andreev. *Sovremennaya elektronika*, **6**, 20 (2014). (in Russian)
- [28] L.M. Fraas, V.S. Sundaram, J.E. Avery, P.E. Gruenbaum, E. Malocsay. *III-V Solar Cells and Doping Processes*. (The patent US5217539A dated 8.06.1993)
- [29] V.M. Andreev, S.V. Sorokina, N.Kh. Timoshina, V.P. Khvostikov, M.Z. Shvarts. *Semiconductors*, **43** (5), 668 (2009). DOI: 10.1134/S1063782609050236
- [30] R.G. Wilson, F.A. Stevie, C.W. Magee. *Secondary Ion Mass Spectrometry: A Practical Handbook for Depth Profiling and Bulk Impurity Analysis* (Wiley, NY., 1989)
- [31] CIAAW. *Isotopic Compositions of the Elements* (2021). Available online at <https://www.ciaaw.org/isotopic-abundances.htm>
- [32] B.I. Boltaks. *Diffuziya v poluprovodnikakh* (Fizmatgiz, M., 1961) (in Russian).
- [33] M.A. Green, K. Emery, Y. Hishikawa, W. Warta, E.D. Dunlop. *Prog. Photovolt: Res. Appl.*, **20**, 12 (2012). DOI: 10.1002/pip.2163
- [34] I.S. Matsak. *Metod iekspierimental'naya ustanovka dlya pretsizionnogo izmereniya kgarakteristik shirikooerturnykh puchkov nepreryvnogo lazernogo izlucheniya* (Dis. kand. tekhn. nauk, M., 2019), 152 s. (in Russian)
- [35] M.V. Gorbunkov, P.V. Kostyukov, V.B. Morozov, A.N. Olenin, L.S. Telegin, V.G. Tunkin, D.V. Yakovlev. *Quant. Electron.*, **35** (12), 1121 (2005). DOI: 10.1070/QE2005v035n12ABEH013037

Translated by I.Mazurov